

Loaded Fireballs and the Blast Wave Model of Gamma Ray Bursts

Charles D. Dermer¹, James Chiang^{1,2}, and Markus Böttcher^{1,3}

ABSTRACT

A simple function for the spectral power $\nu L(\nu) \equiv P(\epsilon, t)$ is proposed to model, with 9 parameters, the spectral and temporal evolution of the observed nonthermal synchrotron power flux of GRBs in the blast wave model. Assumptions and an issue of lack of self-consistency are spelled out. The spectra are found to be most sensitive to the baryon loading, expressed in terms of the initial bulk Lorentz factor Γ_0 , and an equipartition term q assumed to be constant in time. Expressions are given for the peak spectral power $P_p(t) = P(\epsilon_p, t)$ at the photon energy $\epsilon = \epsilon_p(t)$ of the spectral power peak. A general rule is that the total fireball particle kinetic energy $E_0 \simeq \Pi_0 t_0$, where t_0 is the deceleration time scale and $\Pi_0 = P(\epsilon_p, t_0)$ is the maximum measured bolometric power output in radiation, during which it is carried primarily by photons with energy $\mathcal{E}_0 = \epsilon_p(t_0)$.

For clean fireballs with small baryon loading ($\Gamma_0 \gtrsim 300$), GRBs are intense, subsecond, medium-to-high energy γ -ray events, and are difficult to detect because of inadequate photon counts given the insufficiently large effective areas ($\sim 10^3 \text{ cm}^{-2}$) of $> 100 \text{ MeV}$ γ -ray detectors such as EGRET on *CGRO*. Dirty fireballs ($\Gamma_0 \lesssim 30$) produce transient emissions which are longer lasting and most luminous at X-ray energies and below, but these events are lost behind the glow of the X-ray and lower-energy background radiations except for rare serendipitous detections by pointed instruments. The existence of short, hard GRBs is explained, though perhaps not as a distinct class.

1. Introduction

The relativistic blast wave model of GRBs explains, with a minimum of effort, the characteristic time scales and temporal indices of the prompt and afterglow GRB emissions if the sources of GRBs are at cosmological distances. The absorption line measurements of GRB 970508 (Metzger et al. 1997) indicate that GRBs originate from sources located at cosmological distances. Studies of the fireball/blast wave model noted here are Blandford & McKee (1976), Rees & Mészáros (1992), Piran & Shemi (1993), Mészáros & Rees (1993), Mészáros, Laguna, &

¹E. O. Hulbert Center for Space Research, Code 7653, Naval Research Laboratory, Washington, DC 20375-5352

²NRL/NRC Resident Research Associate

³Department of Space Physics and Astronomy, Rice University, Houston, TX 77005-1892

Rees (1993), Mészáros, Rees, & Wijers (1997), Waxman (1997), and Vietri (1997a). We follow the methods of Dermer & Chiang (1998) and Chiang & Dermer (1998) in this work. Particle masses m_p and m_e are in ergs. Photon energies are in units of m_e .

2. Spectral Power and Spectral Power Flux of GRBs in the Blast Wave Model

GRB emissions are most conveniently described in terms of their measured νF_ν spectral power fluxes. Considering only uncollimated, spherically expanding blast waves, the spectral power $P(\epsilon, t) = \nu L_\nu$ is related to the spectral power flux through the expression $P(\epsilon, t) = 4\pi d_L^2 \nu F_\nu$, where d_L is the luminosity distance. Already this relation is not quite right in that the time-delay from different angular regions of a decelerating blast wave can lead to a glow in the afterglow as the blast wave decelerates into and through the nonrelativistic regime. When $\Gamma \gg 1$, however, the strong Doppler beaming means that the bulk of the observed flux is produced by emission regions within an angle $\theta \lesssim 1/\Gamma$ of the line-of-sight direction.

In this limit, we model the evolving characteristic GRB spectrum with the function

$$P(\epsilon, t) \left[\frac{\epsilon \times \text{ergs}}{\text{s} - \epsilon} \right] = \frac{(1 + v/\delta) P_p(t)}{(\epsilon/\epsilon_p)^{-v} + (v/\delta)(\epsilon/\epsilon_p)^\delta} \quad (1)$$

where, on a νL_ν plot, the rising slope has index v (*upsilon*), and the descending slope has the index δ (*down*). Both v and δ are > 0 . Obviously $P(\epsilon_p, t) = P_p(t)$. Expression (1) applies to the nonthermal synchrotron portion of the spectrum, and more detailed treatments are required to deal with self-Compton (Chiang & Dermer 1998; Panaitescu & Mészáros 1998) and external Compton processes (e.g., Dermer, Sturmer, & Schlickeiser 1997).

The spectral power satisfies the normalization

$$E_0 = \int_0^\infty dt \dot{E}_{\text{rad}}(t) = \int_0^\infty dt \int_0^\infty d\epsilon \epsilon^{-1} P(\epsilon, t) , \quad (2)$$

where E_0 is the total energy in baryons at the end of fireball coasting phase. Thus the radiated power

$$\dot{E}_{\text{rad}} \approx 2(v^{-1} + \delta^{-1})P_p(t) . \quad (3)$$

The existence of a low-energy cutoff in the electron distribution function is reasonable, given that the blast wave sweeps up electrons and protons from the circumburst medium with Lorentz factor Γ in the comoving frame. If an efficient mechanism transfers energy from the protons to the electrons, then the low-energy cutoff of the electron Lorentz factors can reach values as large as

$$\gamma_{e,\text{min}} = \xi_e(m_p/m_e)\Gamma . \quad (4)$$

The term $\xi_e \lesssim 1/2$ is an electron equipartition factor. Synchrotron radiation from the cutoff electron distribution produces a low-energy spectrum with $v = 4/3$ (Katz; Tavani 1996; Katz & Piran 1997).

Fermi processes in the blast wave shock can additionally accelerate a nonthermal component of electrons and protons. If the injection index is steeper than 3, or if the injection index is steeper than 2 and cooling processes are rapid, the νF_ν spectrum falls with $\delta > 0$. It is assumed here that the values of v and δ and, by implication, the underlying particle distributions, do not evolve with time. This is clearly not the case (see Chiang & Dermer 1998 for such a treatment) and particle cooling must be carefully considered for interpretations of and fitting to afterglow spectra. But these details are not so important for the overall energetics of the blast wave's observed emissions considered here.

Another crucial uncertainty of blast wave models is the magnetic field strength H in the comoving blast wave frame. This is commonly given in terms of an “equipartition field” obtained by equating magnetic field energy density with the nonthermal particle energy density of the swept-up particles downstream of the forward shock. Thus H is parameterized by the expression

$$H(\text{G}) = [32\pi m_p n \xi_H(r/4)]^{1/2} \Gamma = 116(n \xi_H(r/4))^{1/2} \Gamma_{300}, \quad (5)$$

where n is the density of the swept-up gas in the stationary frame of the explosion, r is the compression ratio, $\Gamma = 300\Gamma_{300}$, and ξ_H is the magnetic-field equipartition parameter. Field generation through dynamo processes could strengthen H with time; flux-freezing and reconnection could weaken it (e.g., Mészáros, Rees, & Papathanassiou 1994). The choice $\xi_H \sim 1$ does not produce GRB spectral forms similar to those observed, as excessive cooling produces a spectral component with $v \cong 0.5$ (Sari, Piran, & Narayan 1997; Chiang & Dermer 1998). Values of $\xi_H \sim 10^{-4}$ are required to give good fits to GRB spectra during the prompt phase. Although there is no justification for treating ξ_H as time-independent when $\xi_H \neq 1$, we do so here for simplicity.

In a tangled field with mean strength H given by eq.(5), the low-energy electron Lorentz-factor cutoff (4) gives a peak in the spectral power at energy $H\gamma_{e,\min}^2/H_{\text{cr}}$ in the comoving frame, where $H_{\text{cr}} = 4.414 \times 10^{13}$ G. To the observer, this energy is boosted and redshifted by a factor $\approx \Gamma/(1+z)$. Thus the observed peak energy ϵ_p at time t is given by

$$\epsilon_p(t) = \mathcal{E}_0[\Gamma(x)/\Gamma_0]^4 (x/x_0)^{-\eta/2} = 3.0 \times 10^{-8} q \Gamma(x)^4 (x/x_0)^{-\eta/2} / (1+z). \quad (6)$$

The coefficient $(m_p/m_e)^2 (32\pi m_p)^{1/2} / H_{\text{cr}} = 2.97 \times 10^{-8}$ and the observed peak photon energy at $x = x_0$ satisfies the relation $\mathcal{E}_0 = 3.0 \times 10^{-8} q / \Gamma_0^4$. The equipartition term

$$q = [n_0 \xi_H(r/4)]^{1/2} \xi_e^2 \quad (6b)$$

when the interstellar medium is uniform with density n_0 ; otherwise, n_0 is the density at the

deceleration radius

$$x_0 = \left[\frac{(3-\eta)E_0}{4\pi n_0 \Gamma_0^2 m_p} \right]^{1/3}. \quad (7)$$

The term x_0 characterizes the distance at which the blast wave has swept up $1/\Gamma_0$ times the initial baryonic mass of the fireball (Rees & Mészáros 1992; Mészáros & Rees 1993). Here we assume that the density can be parameterized by a power law in distance x from the center of the explosion, so that

$$n(x) = n_0(x/x_0)^{-\eta} \equiv n_0 \chi^{-\eta}. \quad (8)$$

Eq. (7) is valid for $\eta < 3$ and is easily generalized for more complicated radial structure such as one with an inner boundary of the circumburst medium. Corresponding to x_0 is the deceleration time scale in the observer's frame,

$$t_0 = \frac{(1+z)x_0}{\Gamma_0^2 c} = \frac{(1+z)}{c \Gamma_0^{8/3} (2g+1)} \left[\frac{(3-\eta)E_0}{4\pi n_0 m_p} \right]^{1/3}. \quad (9)$$

It is useful to parameterize the evolution of the bulk Lorentz factor of the blast wave by the expression

$$\Gamma(x) = \begin{cases} \Gamma_0, & \text{if } 0 \leq \chi < 1; \\ \Gamma_0 \chi^{-g}, & \text{if } 1 \leq \chi \leq \Gamma_0^{1/g}. \end{cases} \quad (10)$$

The index g refers to the deceleration regime. If very little of the swept-up energy is radiated over time scale on which the blast wave decelerates, then the evolution of the blast wave evolves in the non-radiative (or adiabatic regime) with $g \rightarrow 3/2$. On the other hand, if the bulk of the swept-up energy is promptly radiated away, then the blast wave evolves in the radiative regime with $g \rightarrow 3$.

The dimensionless spatial coordinate $\chi = x/x_0$ is related to the observed time through the expression

$$\chi = \begin{cases} t/t_0, & \text{if } 0 \leq t < t_0 \text{ and } 0 \leq \chi < 1; \\ [(2g+1) \frac{t}{t_0} - 2g]^{1/(2g+1)}, & \text{if } t_0 \leq t \leq \frac{t_0}{2g+1} \left(\Gamma_0^{\frac{2g+1}{g}} + 2g \right) \text{ and } 1 \leq \chi \leq \Gamma_0^{1/g}. \end{cases} \quad (11)$$

The power in swept-up particle kinetic energy in the comoving frame is

$$\dot{E}_{\text{ke}} = m_p c B(x) \Gamma(x) [\Gamma(x) - 1] n(x) A(x) \quad (12)$$

(Blandford & McKee 1976), where $A(x) = A_0 \chi^2 = 4\pi x_0^2 \chi^2$ is the area of the spherical blast wave and $B(x)c = \sqrt{1 - 1/\Gamma(x)^2} c$ is its speed. If ζ is defined as the fraction of swept-up kinetic

energy retained in the comoving frame, then $(1 - \zeta)$ is the fraction that is radiated. As previously discussed, only the emitting region along the line of sight makes a significant contribution to the observed flux in the limit $\Gamma \gg 1$. The observed power is boosted and redshifted by the factor $\Gamma^2/(1+z)^2$ over the radiant power in the comoving frame. Consequently we obtain an expression relating the observed power to the swept-up power, namely

$$\dot{E}_{\text{rad}} \cong \frac{\Gamma^2}{(1+z)^2} (1 - \zeta) \dot{E}_{\text{ke}} \cong (1 - \zeta) m_p c \Gamma^4 n(x) A(x) / (1+z)^2. \quad (13)$$

We have used the approach of Dermer & Chiang (1998) to find that in the regime $1 \ll \chi \ll \zeta \Gamma_0^{1/g}$, the fraction of swept-up energy $(1 - \zeta) = (2g - 3 + \eta)/g$ (see Appendix), and we assume that this holds elsewhere as well. Consequently we derive an expression for the measured bolometric spectral power, given by

$$P_p(t) = \Pi_0 \begin{cases} \chi^{2-\eta}, & \text{if } 0 \leq \chi < 1; \\ \chi^{2-\eta-4g}, & \text{if } 1 \leq \chi < \Gamma_0^{1/g}. \end{cases} \quad (14)$$

The coefficient

$$\Pi_0 = \frac{(2g - 3 + \eta) m_p c \Gamma_0^4 n_0 A_0}{2g(v^{-1} + \delta^{-1})(1+z)^2} = \frac{c(2g - 3 + \eta) \Gamma_0^{8/3}}{2g(v^{-1} + \delta^{-1})(1+z)^2} (4\pi m_p n_0)^{1/3} (3 - \eta)^{2/3} E_0^{2/3} \quad (15)$$

represents the bolometric luminosity (ergs s^{-1}) at the time t_0 of peak power output.

For completeness, we rewrite eq. (6) in the form

$$\epsilon_p(t) = \mathcal{E}_0 \begin{cases} \chi^{-\eta/2} & \text{if } 0 \leq \chi < 1; \\ \chi^{-4g-\eta/2}, & \text{if } 1 \leq \chi < \Gamma_0^{1/g}, \end{cases} \quad (16)$$

where

$$\mathcal{E}_0 = \frac{3.0 \times 10^{-8} q \Gamma_0^4}{(1+z)}. \quad (16a)$$

It is straightforward to determine the time-dependence of $P_p(t)$ and $\epsilon_p(t)$ in different regimes. For the parameterized density distribution (8), the peak spectral power P_p increases $\propto t^{2-\eta}$ for $t \leq t_0$, and $P_p(t) \propto t^{-1-\eta/4}$ and $\propto t^{-(10+\eta)/7}$ in the limiting nonradiative ($g = 3/2$) and radiative ($g = 3$) regimes, respectively, when $t \gg t_0$. The peak photon energy $\epsilon_p(t) \propto t^{-\eta/2}$ when $t \leq t_0$, whereas for $t \geq 1t_0$, $\epsilon_p(t) \propto t^{-(12+\eta)/8}$ and $\propto t^{-(24+\eta)/14}$ in the nonradiative and radiative regimes, respectively. For a uniform medium, $\eta = 0$, the peak photon energy $\epsilon_p(t)$ is constant for $t \leq t_0$, whereas for $t \geq t_0$, $\epsilon_p(t) \propto t^{-3/2}$ and $\propto t^{-12/7}$ in the nonradiative and radiative regimes, respectively.

One can also easily determine the temporal indices measured at a fixed observing energy ϵ by consulting equations (1), (11), (14), and (16). Early time $t_p(\epsilon)$ is before the time when the peak

of the spectral power flux sweeps through the observed energy ϵ . Thus $t_p(\epsilon)$ is found by solving $\epsilon \ll \epsilon_p(t_p)$, which corresponds to $t \ll t_p(\epsilon)$, where

$$t_p(\epsilon) = \frac{t_0}{2g+1} \left[\left(\frac{\epsilon}{\mathcal{E}_0} \right)^{-\frac{2g+1}{4g+\eta/2}} + 2g \right], \quad (17a)$$

we find that

$$P(\epsilon, t) \propto t^\alpha \quad \text{where} \quad \alpha = \begin{cases} 2 - \eta + \frac{\eta v}{2}, & \text{if } t \ll t_0, \\ \frac{2 - \eta(1 - \frac{v}{2}) - 4g(1 - v)}{2g+1}, & \text{if } t \gg t_0. \end{cases} \quad (17b)$$

At late times, $t \gg t_p(\epsilon)$, when the peak photon energy is less than the observing energy,

$$P(\epsilon, t) \propto t^{-\beta} \quad \text{where} \quad \beta = \begin{cases} \eta \left(1 + \frac{\delta}{2} \right) - 2, & \text{if } t \ll t_0, \\ \frac{\eta \left(1 + \frac{\delta}{2} \right) + 4g(1 + \delta) - 2}{2g+1}, & \text{if } t \gg t_0. \end{cases} \quad (17c)$$

Table 1 lists derived temporal slopes for various values of v , δ , and g .

3. Model Spectra

Table 2 gives a list of the parameters which, when combined with eq.(11) and defining equations (14), (15), (16), and (16a) and placed in spectral form (1), makes it easy to calculate model spectra. Figure 1 is such a calculation, with parameters as listed in the figure and called “standard” henceforth. Note the peaking near 5 keV at about 10 seconds into the GRB. This is a bit low for the canonical GRB “Band”-type spectrum (Band et al. 1993), but setting the equipartition term q to unity (Fig. 2) places the peak power output at 5 MeV. In fact, if only q changes, the curves are displaced horizontally by a factor q since only $\epsilon_p(t)$ and not $P_p(t)$ is q -dependent. Fig. 1a represents light curves at different energies for Fig. 1.

In this context, a remark concerning some serious issues regarding lack of self-consistency of the parameter list is in order. The type of radiative regime specified by g essentially gives the fraction of internal energy radiated. If nonthermal synchrotron radiation represents the dominant power drain from the blast wave, then the fraction $2 - g^{-1}(3 - \eta)$ of the incoming swept-up power is being transformed into radiation. This places some demands on the underlying particle distribution and comoving energy densities that are not considered here. A detailed numerical simulation with a self-consistent treatment of plasmoid/blast-wave dynamics is essential (Chiang & Dermer 1998).

The Fig. 1 standard, with $g = 1.6$, is near the non-radiative limit. (If $g = 3/2$, there is no radiation by definition.) Fig. 3 shows the standard parameters but with $g = 2.9$. Because the blast

wave radiates brightly in this regime, its inertia drops more quickly and it has a shorter luminous life than in the cases of Figs. 1 and 2. It differs most from the non-radiative case by having a factor ~ 10 shorter duration of its peak power output which is balanced by an order-of-magnitude greater peak power to radiate the same total energy. Most of this power output is emitted by photons with an order-of-magnitude greater energy.

Figures 4 and 5 show the effects of different baryon loading. For a dirty fireball with $\Gamma_0 = 30$ (Fig. 4), the mean photon energy at the peak power output drops by four orders of magnitude and the peak power output drops by nearly three orders of magnitude. To compensate for the constant total energy output simulated here, the peak power output persists for nearly three orders of magnitude longer in time. In this example, the peak power output arises after 10 minutes at UV energies, and develops into a broadband radiation pulse which evolves to lower energies at later times. Incidentally, this behavior is found in blazar flares (e.g., Marscher & Gear 1985), though a closer examination must be made to see if this model provides an adequate explanation for such phenomena.

The clean fireball example with $\Gamma_0 = 3 \times 10^3$, shown in Fig. 5, displays the opposite behavior. Extremely short pulses of radiation are carried by the highest energy photons. For example, when $\Gamma_0 = 3000$, the peak power output of $\approx 10^{51.5}$ ergs is carried by 500 MeV photons in a burst lasting ~ 10 ms. Again, the total energy remains roughly constant, though it is carried by many fewer much higher-energy photons.

The blast wave model is more robust to changes of n_0 and E_0 than of Γ_0 and q . For a fixed baryon loading fraction giving constant Γ_0 , the overall duration of the GRB is multiplied by a factor $\propto (E_0/n_0)^{1/3}$ as a consequence of the deceleration time scale (see eqs.[9] and [7]). The peak power output changes to compensate for the different duration; thus $P_p(t_0) \propto E_0^{2/3}$ when E_0 varies and n_0 is held constant, and $P_p(t_0) \propto n_0^{1/3}$ when n_0 varies and E_0 is constant (see Eq. [15]).

4. Prospects for Detecting Clean and Dirty Fireballs

of photons collected from a GRB at the mean photon energy of peak power output is roughly given by

$$N_\gamma \approx \frac{\Pi_0 t_0 A_{\text{det}}}{4\pi d_L^2 m_e \mathcal{E}_0}, \quad (18)$$

where A_{det} is the effective area of the detector at energy \mathcal{E}_0 . The deceleration time scale (9) defines the rough duration of peak power output, and eq.(16a) gives the mean photon energy of the peak power output at $t = t_0$. Consequently

$$t_0(\text{s}) = \frac{259}{2g+1} \left(\frac{q}{\mathcal{E}_0} \right)^{2/3} \left[\frac{(3-\eta)(1+z)E_{52}}{n_0} \right]^{1/3}. \quad (19)$$

Recalling the expression for the magnitude of peak power output (eq.[15]), we obtain

$$N_\gamma \approx \frac{4.9 (2g - 3 + \eta)(3 - \eta)E_{52}A_{\text{det}}}{g(v^{-1} + \delta^{-1})(1 + z)(2g + 1)d_{28}^2\mathcal{E}_0} \equiv K_\gamma \frac{E_{52}A_{\text{det}}}{d_{28}^2\mathcal{E}_0(1 + z)}, \quad (20)$$

where $d_{28} = d_L/(10^{28}\text{cm})$. For our standard parameters $\eta = 0$, $v = 4/3$, and $\delta = 0.2$,

$$K_\gamma = \begin{cases} 0.075, & \text{for } g = 1.6; \\ 0.36, & \text{for } g = 2.9. \end{cases} \quad (20a)$$

4a. Clean ($\Gamma_0 \gtrsim 300$) Fireballs

The 100 MeV threshold of EGRET corresponds to $\mathcal{E}_0 \simeq 200$. To produce 100 MeV nonthermal synchrotron photons as a consequence of the low-energy cutoff in the electron distribution function requires fireballs with

$$\Gamma_0 \gtrsim 300q^{-1/4}, \quad (21)$$

and this criterion serves to define the clean fireball regime. The number of photons detected from a clean fireball, given the standard parameters used in eq.(20a), is $N_\gamma \approx E_{52}A_{\text{det}}[\text{cm}^2]/[2700d_{28}^2(1+z)]$ and $N_\gamma \approx E_{52}A_{\text{det}}[\text{cm}^2]/[550d_{28}^2(1+z)]$ for $g = 1.6$ and $g = 2.9$, respectively. Such bursts would have durations $\lesssim 1$ s (eq.[19]), and might therefore be difficult to detect in the *Solar Maximum Mission* data base (Harris & Share 1998). The effective area of EGRET at 100 MeV in the wide field mode (Kurfess et al. 1997) is $\sim 800 \text{ cm}^2$ on-axis and $\sim 400 \text{ cm}^2$ at 20° off-axis, so it might be surprising that no sub-second bursts of gamma rays have been reported (Fichtel et al. 1994; Fichtel & Sreekumar 1997) from some members of the clean fireball class which are located at $z \lesssim 1$.

Three possibilities are advanced to explain why this class of clean fireballs with peak power output near 100 MeV has not been discovered:

- No class of clean fireballs defined by eq.(21) exists.
- Sources of clean fireballs are only found at distances characterized by

$$(1 + z)^{1/2}d_{28} \gtrsim E_{52}^{1/2}A_{1000}^{1/2} \begin{cases} 0.6 & \text{for } g = 1.6 \\ 1.4, & \text{for } g = 2.9 \end{cases}, \quad (22)$$

where $1000A_{1000} \text{ cm}^2$ is the effective collecting area of the detector at $\mathcal{E}_0 \approx 200$.

- Most sources of GRBs detected to date lie farther than the distance characterized by eq.(22).

Points (ii) and (iii) are distinct choices. Point (ii) represents a situation where the evolutionary behavior in cosmic time of clean fireballs differs from that of the loaded fireballs which produce BATSE-type GRBs, for example, due to a different class of sources which produces the clean fireballs. Hence the redshift distribution inferred from the analysis of BATSE GRBs would not generally be the same as that for the clean fireballs, and we need not therefore expect that close ($z \ll 1$) clean fireballs exist.

On the other hand, if the clean fireball class exists and evolves through cosmic time in the same manner as the loaded fireballs, point (iii) imposes a requirement on the redshift z_B of the dimmest BATSE bursts to agree with the failure to detect clean fireballs with EGRET. Very crudely, we can scale the number of clean fireballs which could be detected with EGRET to the BATSE detection rate ($\sim 800 \text{ yr}^{-1}$ full sky) and the EGRET field-of-view ($\sim 1/25$ th of the full sky) and lifetime (≈ 5 yrs). If clean fireballs can only be detected with EGRET within $z \lesssim z_E$, then for EGRET not to have detected at least one member of this class,

$$k_{cf} \times 0.04 \times \left(\frac{z_E}{z_B} \right)^j \times 800 \text{ yr}^{-1} \times 5 \text{ yr} \lesssim 1. \quad (23)$$

The term k_{cf} is a class enhancement factor correcting for the number of clean fireballs relative to the number of loaded fireballs which produce GRBs detectable with BATSE. The exponent j represents a cosmological scaling, and $j = 3$ for Euclidean space. Evolutionary and cosmic expansion effects will introduce modifications to j not considered here. Simply taking $j = 3$, we find that $z_B \gtrsim 5z_E k_{cf}^{1/3}$ for the clean fireballs not to have been detected with EGRET. Noting eq.(22), this implies that the faintest BATSE bursts must lie at $z_B \gtrsim 5$ if there are comparable number of loaded fireballs and clean fireballs which evolve similarly through cosmic time.

Stronger conclusions require a detailed size-distribution study involving the cosmological evolution of GRB sources which demonstrates the compatibility of the observed GRB size distribution with the parameters given above, in particular, $E_{52} \sim 1$ and $z_B \sim 5$. The hypernova scenario (Paczyński 1998; Wijers et al. 1998) requires $E_{52} \sim 10^3$ and might therefore not be compatible with the existence of the clean fireball class unless $k_{cf} \ll 1$. Given the uncertainty in the parameters, it remains an open question whether the larger effective area of the proposed *GLAST* instrument would be adequate for the discovery of the clean fireball class, but a discovery of subsecond bursts of ~ 100 MeV photons from clean fireballs remains a real possibility which, should such an event be detected, is not to be confused with the Hawking radiation from evaporating mini-black holes by virtue of its afterglow behavior.

The class of bursts with hard spectra and short duration (Belli 1995; Kouveliotou et al. 1996) would be explained by fireballs which are less baryon-loaded than the fireballs producing the typical BATSE GRB. The size distribution of this short/hard class of GRBs is found to be more in accord with a $-3/2$ isotropic size distribution than the longer duration GRBs. Fewer photons are emitted from a weakly-loaded fireball, though at higher energies (eq.[20]). Consequently, a smaller number of closer, clean fireballs would be detected in a photon-limited survey, and these

would be found to be more nearly isotropic if there is not significant source evolution of nearby ($z \lesssim 1$) GRB sources. The overall properties of the short/hard class of GRBs therefore appears to be in accord with the fireball model if there is a range of baryon-loading in fireballs. A model for the distribution of baryon loading in terms of distributions of Γ_0 and E_0 is needed to establish whether these GRBs constitute a distinct class or an extension of the typical loaded fireball in the cleaner limit.

Because gamma-ray telescopes are essentially photon counters, it is easy to see from eq. (20) that larger effective areas and larger fields-of-view are required to detect clean fireballs. Following the analysis leading to eq.(23) for COMPTEL parameters (see, e.g., Hanlon et al. 1995) leads to similar conclusions as in the EGRET analysis above, noting the smaller effective area ($\sim 10^2$ cm 2) of COMPTEL on *CGRO*. Nonetheless, a search of the COMPTEL data base for GRBs not detected with BATSE will provide additional constraints on the number and redshift distribution of relatively clean (i.e., $100 \lesssim \Gamma_0 \lesssim 300$) fireballs.

4b. Dirty ($\Gamma_0 \lesssim 30$) Fireballs

When the baryon-loading gets large and Γ_0 gets small, the peak power output plummets $\propto \Gamma_0^{8/3}$ (eq.[15]). For a given total energy, the deceleration time scale increases $\propto \Gamma_0^{8/3}$ so that $\Pi_0 t_0 \approx E_0$. The peak photon energy \mathcal{E}_0 decreases $\propto \Gamma_0^4$. Because a large number of X-ray telescopes operate near 10 keV, we can use $\mathcal{E}_0 \sim 10/511$ to define the dirty fireball regime, which includes those blast waves with

$$\Gamma_0 \lesssim 30q^{-1/4} \quad (24)$$

(compare eq.[21]).

Gamma-ray telescopes at $\gg 10$ MeV energies are generally photon-limited, whereas X-ray telescopes are generally background limited. A signal of N_γ counts given by eq.(18) is detected above a background of B_G counts at significance $\geq n_\sigma$ provided that

$$N_\gamma \gtrsim n_\sigma (2B_G)^{1/2} . \quad (26)$$

The number of background counts

$$B_G \cong \Delta\epsilon_{\text{det}} \cdot \dot{\Phi}_{\text{dif}}(\Omega, \epsilon_{\text{det}}) \cdot \Delta\Omega \cdot \Delta t \cdot A_{\text{det}} , \quad (27)$$

where, from right to left, the terms are the detector area, the observing time, the field-of-view (FoV) of the detector, the diffuse photon flux weighted by an average photon energy within the band, and the bandwidth. The diffuse background is composed of instrumental, magnetospheric, zodiacal, Galactic, and extragalactic components, which are time-independent in general. Here we

give a background estimation for X-ray telescopes considering only the diffuse extragalactic X-ray background, which provides a lower limit to B_G .

In the 3-100 keV range, Boldt (1987) gives the expression

$$\epsilon \dot{\Phi}_{\text{XRB}}(\epsilon, \Omega) \left[\frac{\text{ph}}{\text{cm}^2 \text{s}} \right] \cong 5.6 \left[\frac{E(\text{keV})}{3 \text{ (keV)}} \right]^{-0.29} \exp[-E(\text{keV})/40 \text{ keV}] \quad (28)$$

for the diffuse extragalactic X-ray background flux. At 3 keV, corresponding roughly to the mean energy of photons detected by an X-ray telescope sensitive in the 1-10 keV band, the diffuse flux is $\simeq 5 \text{ ph cm}^{-2} \text{ s}^{-1} \text{ sr}^{-1}$.

Substituting eqs.(20) and (27) into eq.(26) with the stated diffuse flux gives the result that detection at the n_σ level requires an X-ray telescope with

$$\frac{A_{\text{det}}}{\Delta\Omega} \left[\frac{\text{cm}^2}{\text{sr}} \right] \gtrsim \frac{3.6 \times 10^{-4} d_{28}^4 n_\sigma^2 (1+z)^2 \Delta t}{K_\gamma^2 E_{52}^2 f(\Delta t/t_0)} \quad (29)$$

The function $f(y) = y^2$ for $y \leq 1$, and $f(y) = 1$ for $y > 1$. The detection efficiency is clearly optimized when $\Delta t \approx t_0$. The deceleration time scale for a burst peaking at $\mathcal{E}_0 \cong 3/511 = 0.006$ implies, from eq.(16a), that $\Gamma_0 \cong 21(1+z)^{1/4}/q^{1/4}$. Because q is constrained to be \lesssim unity, a model burst peaking at 3 keV limits from below the value of Γ_0 . The deceleration time scale at this energy is

$$t_0(3 \text{ keV}) \simeq 8000 \frac{(1+z)^{1/3} q^{2/3}}{2g+1} \left[\frac{(3-\eta)E_{52}}{n_0} \right]^{1/3} \text{ sec}, \quad (30)$$

When $\eta = 0$, one obtains the requirement that for a n_σ detection,

$$\frac{A_{\text{det}}}{\Delta\Omega} \gtrsim \frac{d_{28}^4}{E_{52}^{5/3} n_0^{1/3}} q^{2/3} \left(\frac{n_\sigma}{5} \right)^2 (1+z)^{7/3} \begin{cases} 4300, & \text{for } g = 1.6; \\ 120, & \text{for } g = 2.9. \end{cases} \quad (31)$$

for an X-ray telescope to be able to detect a dirty fireball. Typical X-ray detectors have effective areas $\sim 10^2 \text{ cm}^2$ (see Table 3 for general specifications of some X-ray telescopes used to detect GRBs), so we scale to a detector of area $100A_{100} \text{ cm}^2$. To detect dirty fireballs at $z \approx 1$, the diffuse X-ray background means that it is necessary for the detector's FoV

$$\Delta\Omega \lesssim \frac{E_{52}^{5/3} A_{100}}{q^{2/3} (n_\sigma/5)^2} \begin{cases} 0.0045, & \text{for } g = 1.6; \\ 0.16, & \text{for } g = 2.9. \end{cases} \quad (32)$$

Thus the X-ray detector has to have a FoV $\lesssim 4^\circ \times 4^\circ$ or $\lesssim 20^\circ \times 20^\circ$ to detect dirty fireballs at $z \sim 1$, depending on whether the blast decelerates primarily in the non-radiative or radiative regimes, respectively. Fireballs at $z \lesssim 1$ place much weaker constraints on the detector's FoV, as indicated in equation (31), and then it becomes a question of the number of such sources one could expect to see.

Small field-of-view instruments will only detect an X-ray flash from a dirty fireball very rarely unless the class of dirty fireballs is populous. Given that there are ~ 800 BATSE-detectable GRBs per year averaged over the full sky, this implies a chance probability of $\sim 0.02 \cdot k_{df} \cdot k_d^2$ per year for a detector with a $k_d^\circ \times k_d^\circ$ FoV. Since the class enhancement factor k_{df} of dirty fireballs compared to loaded BATSE/GRB fireballs is not known at all, it is quite speculative to suppose that a narrow FoV X-ray or optical telescope would happen upon a GRB without it being directed there. On the other hand, it is not unreasonable for this to happen occasionally. Moreover, there would be no difficulty in detecting dirty fireballs at $z \lesssim 1$, but the rate of such events is proportionally smaller by the volume factor in addition to cosmic expansion and evolutionary factors.

More concrete deductions about the probability of serendipitously detecting X-ray flashes from dirty fireballs requires a size distribution study tied to a particular detector's characteristics. Our analysis indicates that it is feasible that some of the X-ray flashes observed in archival searches of *Einstein* (Connors, Serlemitsos, & Swank 1986) and *ROSAT* PSPC (Li et al. 1998; Sun et al. 1998) data are emissions from dirty fireballs only if $k_{df} \gg 1$, given that the effective FoV of the *ROSAT* PSPC is $\sim 1^\circ \times 1^\circ$. Whether this conflicts with the Beppo-SAX WFC detection rate of X-ray flashes requires further study beyond the simple estimates presented here. A comparison between detection rates or upper limits of flashes is important given that one can use such studies to constrain the density distribution of dirty fireballs, and to determine the optimal characteristics of a burst detector for searching for such fireballs.

5. Discussion

A slewing strategy such as the one so successfully demonstrated by the Beppo-SAX team and collaborators (e.g. Costa et al. 1997; van Paradijs et al. 1997; Piro et al. 1998a,b) opens rich possibilities for discoveries which must be carefully weighed in GRB telescope design. Here we have attempted to provide an exposition of the blast wave model that provides a simple way to model the evolving spectral power fluxes, and which furthermore helps us to understand dedicated and serendipitous GRB observations. Eq.(1) is the proposed time-dependent spectral form. It employs the 9 parameters listed in Table 2 that follow from the basic blast wave model. Its crucial underlying assumptions are that the photon indices ν and δ and the equipartition term q are constant in time. Over this looms a question of lack of self-consistency, since specification of the radiative regime g constrains the magnetic field and photon energy densities and particle distributions to produce the requisite radiative power. A numerical code with self-consistent treatment of plasmoid dynamics (e.g., Chiang & Dermer 1998) is required for detailed studies.

In spite of these concerns, eq.(1) can be easily employed to make estimations of imaging capabilities of burst detectors given slewing rates of narrow field instruments toward a cosmic transient. It can be used to calculate photoelectric absorption variations in the GRB environment and its imprint upon the observed burst spectrum (work in preparation by the authors). It can also, of course, be used to model the temporal behavior of GRB spectra.

By displaying the spectral power flux in the form of eq.(1), we obtained an important rule relating observed bolometric luminosities, characteristic durations, and characteristic photon energies at the peak of the spectral power output of fireballs. The characteristic time scale over which the bulk of the power is radiated is the deceleration time scale t_0 (eq.[9]; Rees & Mészáros 1992), and $t_0 \propto \Gamma_0^{-8/3}$, where Γ_0 specifies the baryon loading. The peak power output Π_0 (eq.[15]) is also $\propto \Gamma_0^{8/3}$. Because most of the total particle kinetic energy, E_0 , originally in the fireball during its coasting phase is radiated during the observed time t_0 , we have

$$E_0 \approx \Pi_0 t_0 . \quad (33)$$

Moreover, the bulk of this energy is observed in the form of photons with characteristic energy \mathcal{E}_0 given by eq.(16a); note that $\mathcal{E}_0 \propto q\Gamma_0^4$.

Fig. 6 shows the variation of Π_0 and t_0 for a range of Γ_0 outlining the loaded fireball regime $30 \leq \Gamma_0 \leq 300$, and the dependence of these parameters on variations in E_{52} and n_0 . The inset shows the dependence of \mathcal{E}_0 on Γ_0 for this range of Γ_0 when q varies from 1 to 10^{-4} . The overall energetics, powers, and time scales of fireballs in different regimes of baryon-loading can be determined from this figure.

We used eq.(33) to determine the prospects for detecting fireball emissions at other photon energies. Benchmark characteristics of X-ray, soft gamma-ray, and medium-energy gamma-ray telescopes were used to establish criteria for clean, loaded, and dirty fireballs. Detection of clean fireballs at $\gtrsim 100$ MeV energies implies $\Gamma_0 \gtrsim 300$, and the detection of dirty fireballs at $\lesssim 10$ keV energies implies $\Gamma_0 \lesssim 30$ (neglecting for now the weak dependence on the equipartition term q). The clean fireball class was not discovered with EGRET; this means either that there are no sources of energetic clean fireballs, or that the energies and z -dependent bursting rates of clean fireballs are such that previous > 100 MeV detectors have not had the exposure time and sensitivity to detect these sources. The prospect of such a discovery with *GLAST* remains real.

This is a good place to qualify our use of eq.(33) which gives the general observational properties of fireballs with different baryon loading parameters, and the implied prospects for detecting such fireballs. EGRET has, of course, detected > 100 MeV gamma-ray emission from GRBs detectable with BATSE from the loaded ($30 \lesssim \Gamma_0 \lesssim 300$) fireball class. Many of these types of sources will undoubtedly be detected with the *GLAST* mission as well. But the > 100 MeV and GeV photons detected to date (e.g., Hurley et al. 1994; Dingus 1995) are not those produced by the electrons near the low-energy cutoff of the electron distribution function. These photons are much more likely to be the synchrotron self-Compton emission (e.g., Chiang & Dermer 1998) or the nonthermal synchrotron radiation from ultra-high energy protons (Vietri 1997b; Böttcher & Dermer 1998) accelerated in the loaded fireball blast wave. These emissions are distinguished by their slow decay, which explains why EGRET detects this emission long after the main portion of the BATSE burst has decayed. What EGRET has not discovered, but is predicted by the blast wave model, is a class of clean fireballs which produces a luminous subsecond burst of $\gg 100$ MeV

radiation.

Besides clean fireballs, we also used eq.(33) to provide observable characteristics of dirty fireballs. Because the peak luminosities and mean photon energy at the peak of power output are lower in dirtier fireballs, the diffuse sky backgrounds make detection of such a class of objects by wide-field instruments problematic. On the other hand, the expected rate of detection of dirty fireballs by pointed instruments with a few square degree FoV is very unlikely unless the rate of dirty fireball explosions greatly exceeds the rate of loaded BATSE/GRB fireballs. Whether any member of this class has been discovered is uncertain, though X-ray flashes have indeed been detected in the *Einstein* and *ROSAT* data bases.

The optimal design of a GRB mission, given our present understanding of loaded fireballs and GRB blast waves, would therefore seem to employ a hard X-ray/soft gamma-ray burst detector and a narrow FoV X-ray telescope which can rapidly slew to that position. But more exciting still would be to design instruments which additionally discover the sister classes of clean and dirty fireballs predicted by the fireball model of GRBs.

The work of CD was supported by the Office of Naval Research and the *Compton Gamma Ray Observatory* Guest Investigator Program. CD thanks Jim Kurfess, Neil Johnson, and Mark Strickman for enlightening discussions. The work of JC was performed while he held a National Research Council - Naval Research Laboratory Associateship. MB acknowledges support by the German Academic Exchange Service (DAAD).

Appendix A. The Fraction of Radiated Energy

In order to find the relation between the fraction ζ of swept-up energy retained in the blast wave to the rate of deceleration of the blast wave, described by the power-law index g in the asymptotic regime $x \gg x_0$. We start from the equation of conservation of momentum (Eq. [6] of Dermer & Chiang [1998]) and note that the energy in swept-up particles accumulated up to the point x is

$$\int_0^\infty dp \gamma N_p(\gamma) = \int_0^x d\tilde{x} n_{\text{ext}}(\tilde{x}) A(\tilde{x}) [\zeta \Gamma(\tilde{x}) + (1 - \zeta)]. \quad (\text{A1})$$

In the asymptotic regime $x_0 \ll x \ll x_{\text{tr}}$, where $x_{\text{tr}} = x_0 \Gamma_0^{1/g}$ and $1 \ll \Gamma(x) = \Gamma_0 \left(\frac{x}{x_0}\right)^{-g}$, this yields

$$-\frac{\Gamma'(x)}{\Gamma^2(x)} = \frac{g}{x \Gamma(x)} \approx \frac{n_0 A_0 \left(\frac{x}{x_0}\right)^{2-\eta}}{N_{\text{th}} + n_0 A_0 \left[\Gamma_0 \zeta \int_{x_0}^x d\tilde{x} \left(\frac{\tilde{x}}{x_0}\right)^{2-g-\eta} + (1-\zeta) \int_0^x d\tilde{x} \left(\frac{\tilde{x}}{x_0}\right)^{2-\eta} \right]}. \quad (\text{A2})$$

The denominator on the right-hand side of Eq. (A2) is dominated by the first integral, unless the blast wave is in the extreme radiative regime. Thus, if $x \ll \zeta x_{\text{tr}}$, Eq.(A2) becomes

$$\frac{g}{\Gamma_0 x_0} \left(\frac{x}{x_0}\right)^{g-1} \approx \frac{3-g-\eta}{\zeta \Gamma_0 x_0} \left(\frac{x}{x_0}\right)^{g-1}, \quad (\text{A3})$$

or

$$\zeta = \frac{3-g-\eta}{g}. \quad (\text{A4})$$

Table 1: Slopes of the Temporal Evolution of the Flux at Fixed Photon Energy when $t \gg 0$

slope	g	$v = 1$	$v = 4/3$						
α	1.6	0.48	0.98						
α	2.9	0.29	0.86						
		$\delta = 0$	$\delta = 1/5$	$\delta = 1/3$	$\delta = 1/2$	$\delta = 3/4$	$\delta = 1$	$\delta = 2$	
β	1.6	1.05	1.35	1.56	1.81	2.19	2.57	4.09	
β	2.9	1.41	1.75	1.98	2.26	2.69	3.12	4.82	

Table 2: Parameters for Model of Evolving GRB Spectral Power Flux

Parameter	Description
Γ_0	initial Bulk Lorentz factor
q	equipartition term
g	index of Γ evolution
E_0	total particle kinetic energy in GRB
v	spectral index of rising portion of νL_ν spectrum
δ	spectral index of decaying portion of νL_ν spectrum
z	cosmological redshift
n_0	density at $x = x_0$
η	index of density distribution

^aergs cm⁻² s⁻¹

^bLarge Area Detectors; 10 s GRB

^cBeppo-SAX data from homepage; see also Piro et al. 1998

REFERENCES

Band, D. L., et al. 1993, ApJ, 413, 281
 Belli, M. 1995, Ap&SS, 231, 43
 Boldt, E. 1987, Physics Reports, 146, no. 4, 215
 Böttcher, M., & Dermer, C. D. 1998, ApJL, in press (astro-ph 9801027)
 Blandford, R. D., & McKee, C. F. 1976, Phys. Fluids, 19,1130
 Chiang, J., & Dermer, C. D. 1998, ApJ, submitted (astro-ph 9803339)
 Connors, A., Serlemitsos, P., & Swank, J. H. 1986, ApJ, 303, 769
 Costa, E., et al. 1997, Nature, 387, 783
 Dingus, B. L. 1995, A&SS, 231, 187
 Dermer, C. D., & Chiang, J. 1998, New Astronomy, 3, 157

Table 3: Characteristics of Operating Missions with GRB Detectors

	Energy band (keV)	FoV	Effective Area (cm ²)	Sensitivity ^a	imaging
CGRO BATSE	50 – 300	4π		6×10^{-8} ^b	few degrees
SAX GRBM	40 – 700	$20^\circ \times 20^\circ$	120		$10' \rightarrow 3'$
SAX WFC	1.5 – 26	$20^\circ \times 20^\circ$	120	$\sim 10^{-10}$ in 10^3 s ^c	$10' \rightarrow 2'$
SAX NFI LECS	0.1 – 10	0.5°	22@0.25 keV	$\sim 3 \times 10^{-14}$ in 10^5 s	50''
SAX NFI MECS	0.1 – 10	0.5°	150@6 keV		

Dermer, C. D., Sturner, S. J., & Schlickeiser, R. 1997, ApJS, 109, 103

Fichtel, C. E., & Sreekumar, P. 1997, in The Fourth Compton Symposium, ed. C. D. Dermer, M. S. Strickman, & J. D. Kurfess (New York: AIP), 436

Fichtel, C. E., et al. 1994, ApJ, 434, 557

Harris, M. J., & Share, G. J. 1998, ApJ, in press

Hanlon, L. et al., 1995, A&SS, 231, 157

Hurley, K. C., et al. 1994, Nature, 372, 652

Katz, J. I. 1994, ApJ, 432, L107

Kouveliotou, C., et al. 1996, in AIP Conf. Proc. 384, Third Huntsville Workshop on Gamma-Ray Bursts, ed. C. Kouveliotou, M. S. Briggs, & G. J. Fishman (New York: AIP), 42

Katz, J. I., & Piran 1997, ApJ, 490, 772

Kurfess, J. D., Bertsch, D. L., Fishman, G. J., & Schönfelder, V. 1997, in The Fourth Compton Symposium, ed. C. D. Dermer, M. S. Strickman, & J. D. Kurfess (New York: AIP), 509

Li, H., Sun, X., Fenimore, E. E., & Wang, Q. D., in the Fourth Huntsville Gamma-Ray Burst Symposium, in press

Marscher, A. P., & Gear, W. K. 1985, ApJ, 298, 114

Mészáros, P., & Rees, M. J. 1993, ApJ, 405, 278

Mészáros, P., Laguna, P., & Rees, M. J. 1993, ApJ, 415, 181

Mészáros, P., Rees, M. J., & Papathanassiou, H. 1994, ApJ, 432, 181

Mészáros, P., Rees, M. J., & Wijers, R. A. M. J., 1997, ApJ, submitted (astro-ph/9709273)

Metzger, M. R., et al. 1997, Nature, 387, 878

Paczynski, B. 1998, ApJ, L45

Panaitescu, A., & Mészáros, P. 1998, ApJ, 492, 683

Piro, L., et al. 1998, A&A, 331, L41

Piro, L., et al. 1998, A&A, 329, 906

Piran, T., & Shemi, A. 1993, ApJ, 403, L67

Rees, M. J., & Mészáros, P., 1992, MNRAS, 258, 41P

Sari, R., Piran, T., & Narayan, R. 1997, astro-ph 9712005

Sun, X., Li, H., Fenimore, E. E., & Wang, Q. D., in the Fourth Huntsville Gamma-Ray Burst Symposium, in press

Tavani, M. 1997, ApJ, 483, L87

van Paradijs, J., et al. 1997, Nature, 386, 686

Vietri, M. 1997a, ApJ, 478, L9

Vietri, M. 1997b, PRL 78, 23, 4328

Waxman, E. 1997, ApJ, 485, L5

Wijers, R. A. M. J., Bloom, J. S., Bagla, J. S., & Natarajan, P. 1998, MNRAS,

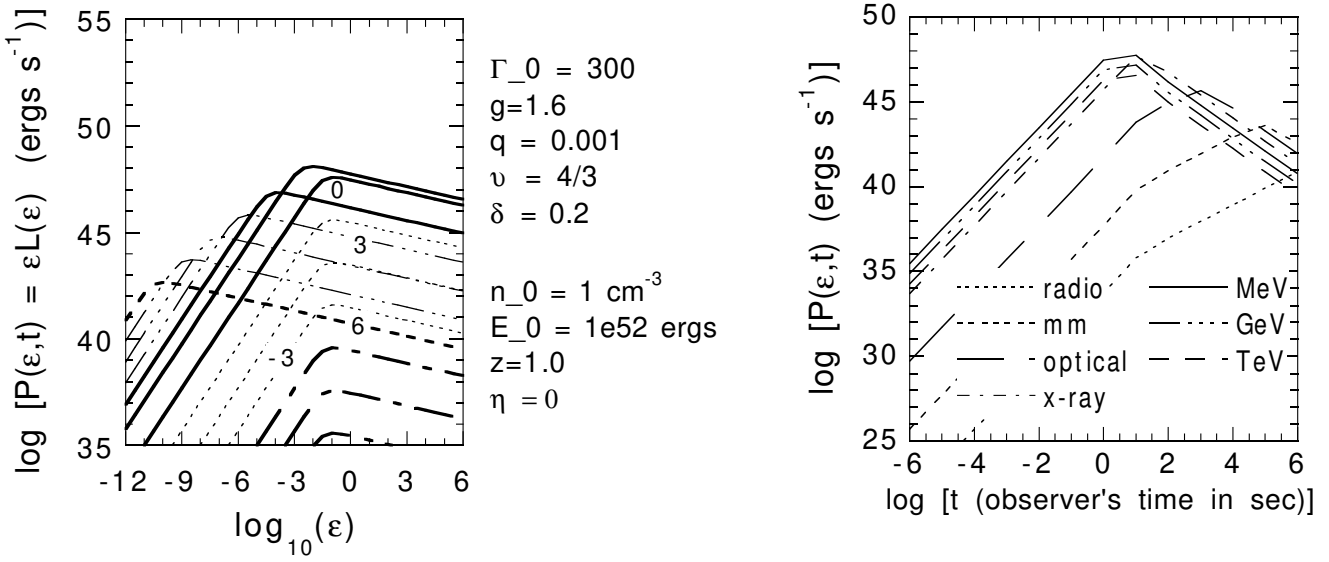


Fig. 1.— a) Evolution of the GRB radiation using our standard parameters $\Gamma_0 = 300$, $g = 1.6$, $q = 10^{-3}$, $v = 4/3$, and $\delta = 0.2$. The curves are labeled by the base 10 logarithm of the observer's time in s. The time evolution is given by the increase of flux $\propto t_{\text{obs}}^2$ with constant peak photon energy early during the burst and the power-law decay of the flux with decreasing peak photon energy in the later phase: thick dot-dashed \rightarrow thin dashed \rightarrow thick solid \rightarrow thin triple-dot dashed \rightarrow thick dashed curves. b) GRB light curves in different energy bands resulting from the evolution shown in frame a).

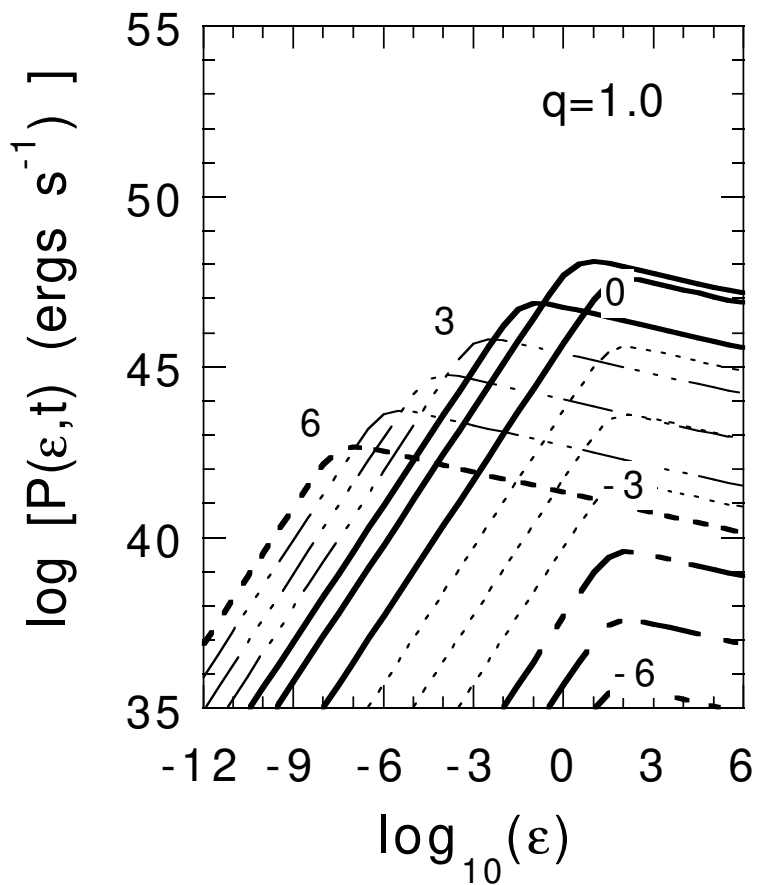


Fig. 2.— Same as Fig. 1a, but with equipartition parameter $q = 1$.

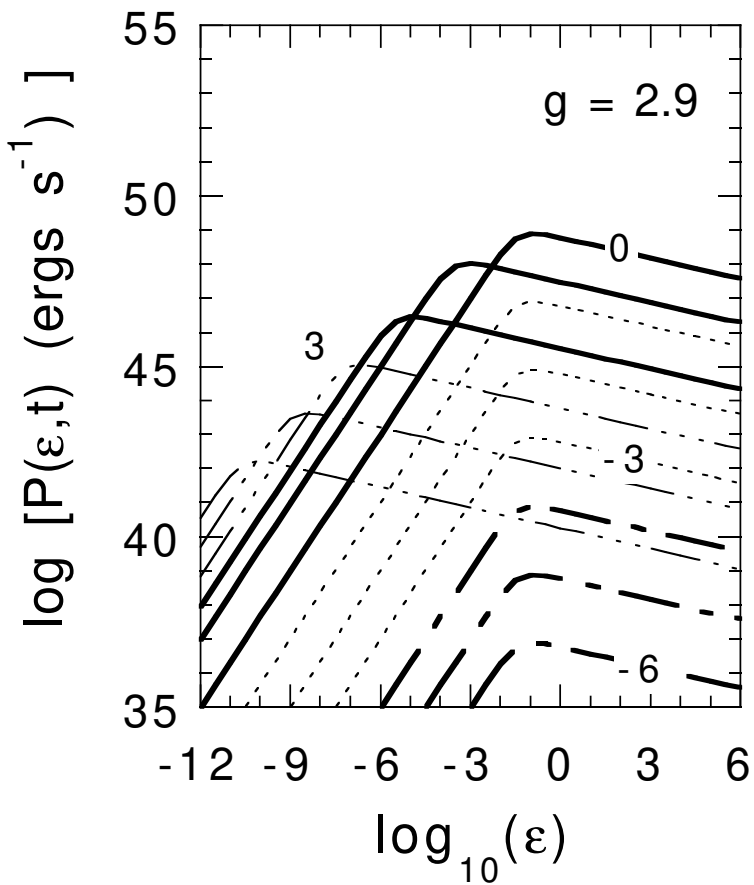


Fig. 3.— Same as Fig. 1a, but for a blast wave in the radiative regime ($g = 2.9$).

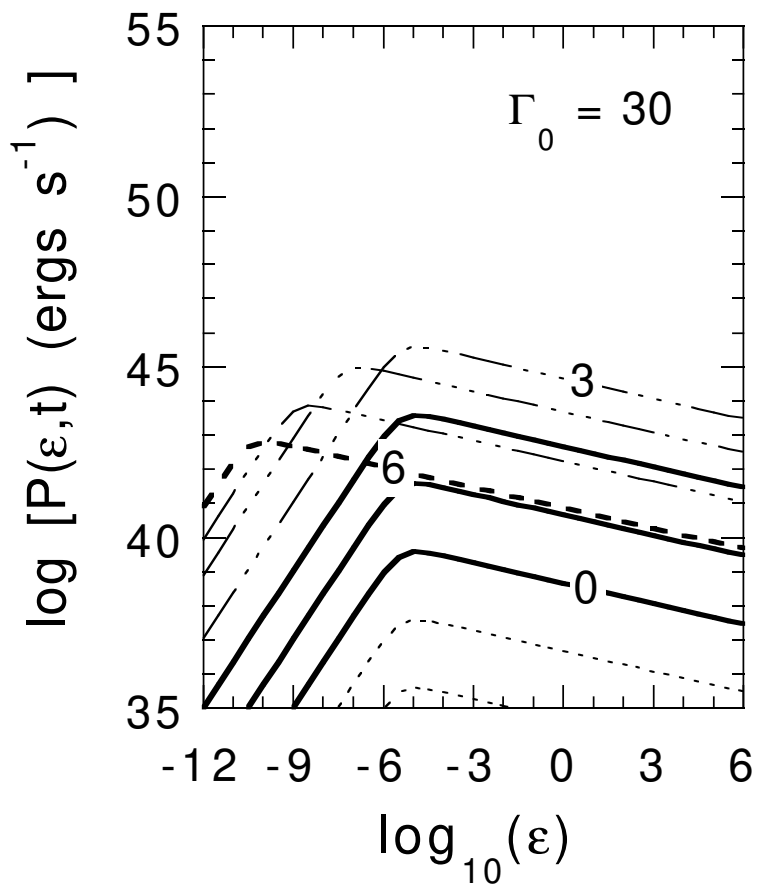


Fig. 4.— Same as Fig. 1a, but for a dirty fireball with $\Gamma_0 = 30$.

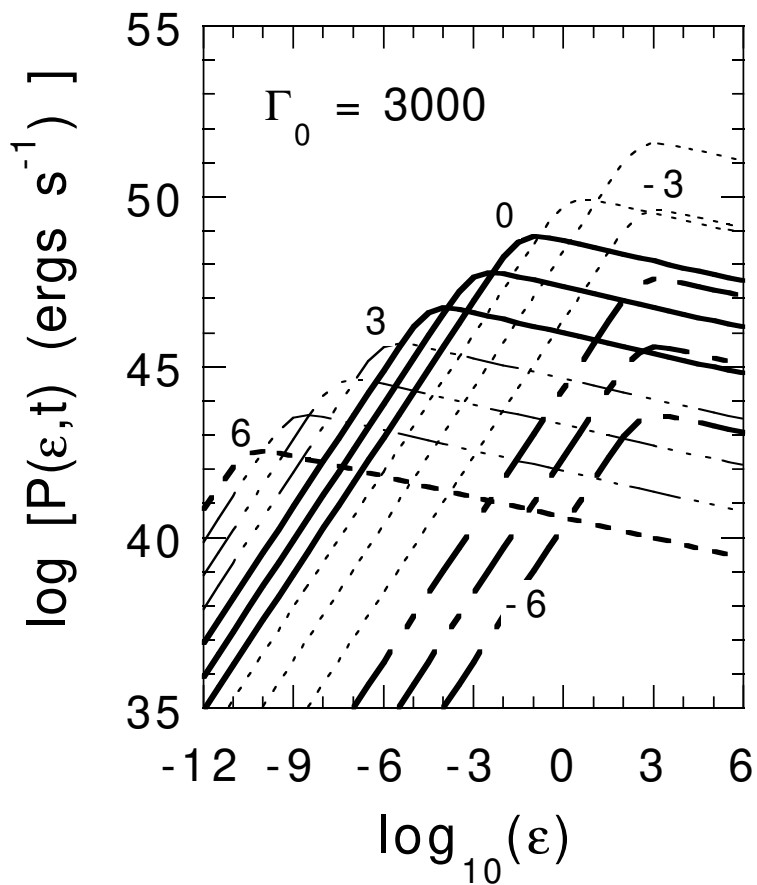


Fig. 5.— Same as Fig. 1a, but for a pure fireball with $\Gamma_0 = 3000$.

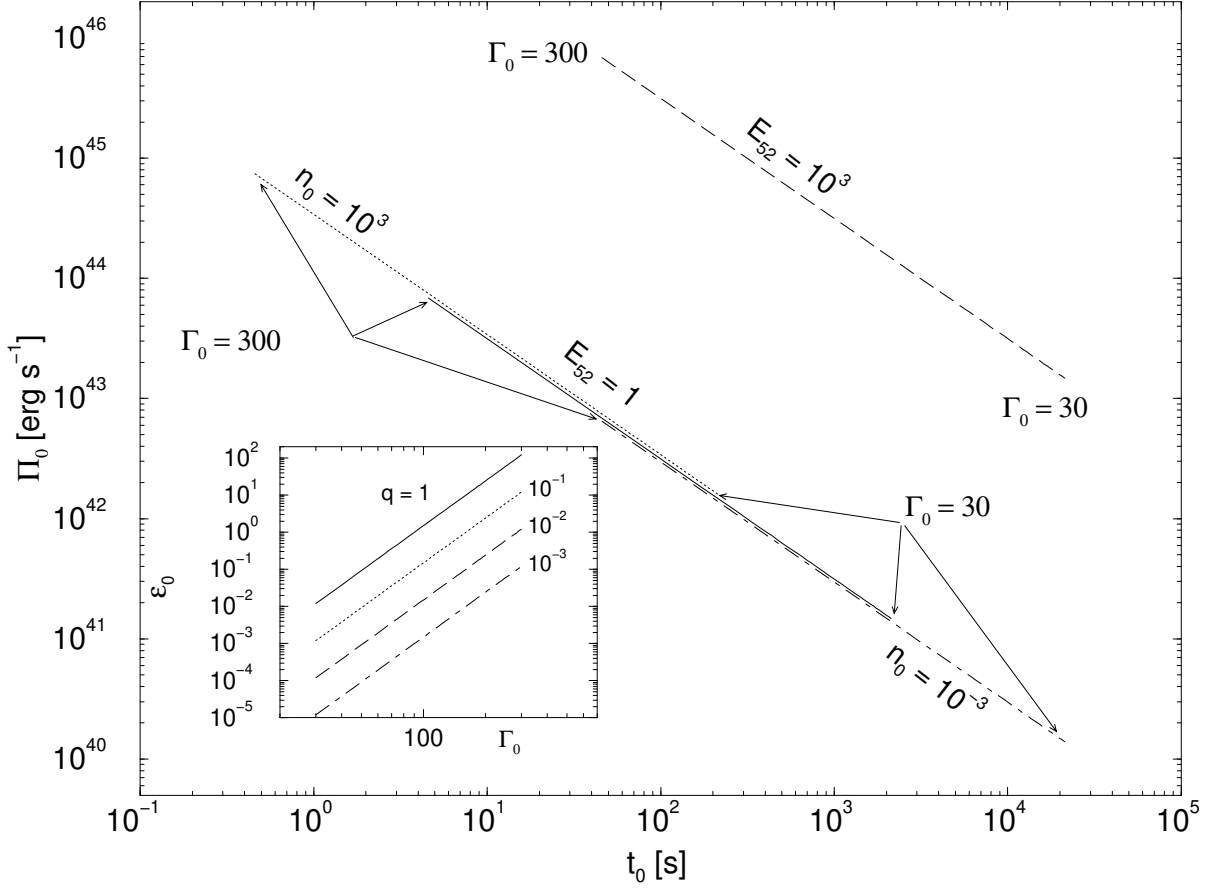


Fig. 6.— Dependence of the fundamental observables Π_0 , t_0 and ϵ_0 on the baryon loading (represented by Γ_0), the total explosion energy $E = 10^{52}E_{52}$ erg s $^{-1}$ and the external density n_0 cm $^{-3}$.